Experimental Techniques (2018) 42:355–369
https://doi.org/10.1007/s40799-018-0239-0

Strengthening of Old Masonry Walls for out-of-Plane Seismic Loading with a CFRP Reinforced Render

J. Guerreiro[1] · J. G. Ferreira[1] · J. Proença[1] · A. Gago[1]

Received: 25 March 2017 / Accepted: 7 February 2018 / Published online: 21 February 2018

Abstract
This paper presents part of the results of an experimental campaign for the development of a strengthening technique, aimed at retrofitting old buildings by the application of exterior reinforcing render layers to their masonry walls. The experimental campaign comprised tests with out-of-plane loading on both strengthened and non-strengthened masonry walls. The strengthening layer material, hereby designated as CFRP (Carbon Fibre Reinforced Polymer) reinforcing render, is an innovative material for the seismic retrofitting of masonry walls. The reinforcing render material consists of a lime-based mortar reinforced with a carbon fibre mesh, applied on one or both facings of a masonry wall. This solution was developed to provide the masonry wall with improved mechanical properties, while respecting the main principles for a proper rehabilitation of old buildings.

Keywords Masonry walls · Seismic loading · Out-of-plane behaviour · Reinforced render · CFRP

Introduction

The strengthening technique described in the present paper was designed with the purpose of preventing the out-of-plane collapse of masonry walls in old buildings during earthquakes, thus ensuring a better overall structural behaviour.

For the proper structural behaviour of a masonry building, every wall should resist actions perpendicular to its plane, avoiding collapse by bending or overturning. Several authors have reported the damage pattern of old buildings subjected to real earthquakes [1–4] particularly observing their masonry walls crack patterns [5–9]. This surveys show that the most frequent (and fragile) failure mechanism is the out-of-plane collapse of the main facade, often involving portions of perpendicular walls connected to it. Therefore, a satisfactory seismic behaviour will only be achieved if the out-of-plane collapse is prevented while the walls working in their own plane absorb and resist most of the inertia forces developed in an earthquake.

The mechanism that leads to the out-of-plane collapse of exterior walls involves the rigid body rotation of the wall (or of a portion of it) around a horizontal joint [5, 10–12], induced by the inertia forces generated by an earthquake.

In the worst case, the wall is loose at the top (without any restriction) and is disconnected from the orthogonal walls. In these cases, a vertical cantilever mechanism [13] is initiated when the feeble connections at the floor levels also get loose.

For old buildings with effective connections between walls and floors, the former mechanism is not so common. In these cases, the most frequent failure mechanisms are of two types. One of them involves the horizontal bending of the wall, supported at their extremities by the perpendicular walls [14, 15]. The other consists of the wall vertically bending between floors. The first mechanism is recognized by vertical crack patterns while the second by the development of horizontal cracks [10, 16]. The overall damage pattern is usually rather complex, depending on the connections effectiveness and the floors stiffness, and usually involves both types of mechanisms (vertical and horizontal bending), leading to a more complex crack pattern where diagonal cracks may be predominant. In the case of multi-layer type walls, collapse may only engage the outer panel of the wall, with a significant decrease in the seismic strength.

The overturning of a wall that interacts with orthogonal ones at building corners usually ends up damaging the latter in their planes [10, 17]. Such interaction usually implicates the facade collapse and the diagonal cracking of the orthogonal walls.

The seismic strengthening of an ancient masonry building involves the prevention of different failure mechanisms [18].

✉ J. Guerreiro
jg@civil.ist.utl.pt

[1] Universidade de Lisboa Instituto Superior Tecnico, Lisbon, Portugal

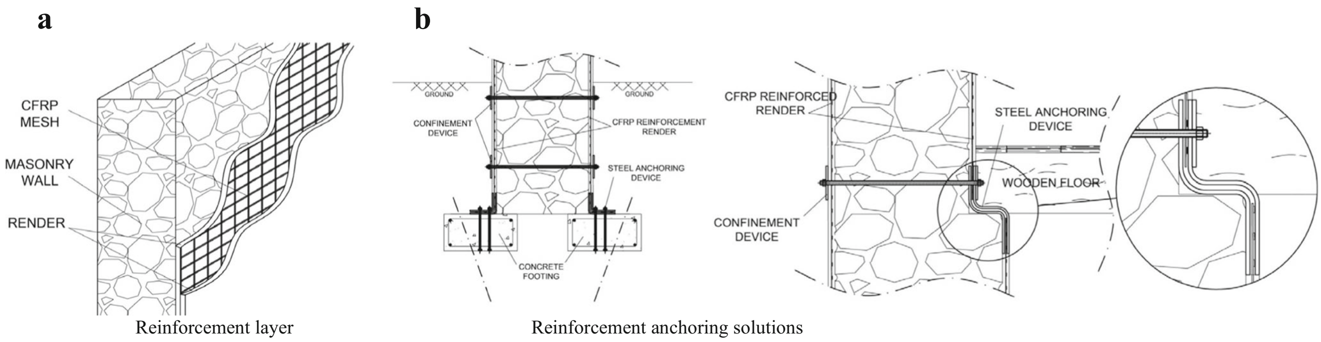

Fig. 1 Strengthening technique

The critical failure mechanism is often associated with the out-of-plane collapse of the façade walls, as it occurs for lower seismic loading. In this sense, the out-of-plane strengthening of masonry walls is mandatory in the context of seismic rehabilitation [19].

Description of the Strengthening Technique

The developed strengthening technique consists of the application of a CFRP reinforcing render on the masonry walls substrate (Fig. 1a). Such a layer is endowed with high tensile strength and bonding capacity to the original masonry substrate, providing the masonry with improved bending resistance.

The reinforcing render can be described as a bi-component material, composed by a hydraulic but non-cementitious coating mortar and a carbon fibre reinforced polymer (CFRP) mesh. The coating mortar's function is to bond the reinforcement layer to the masonry wall, as it retains chemical, physical and mechanical compatibility with the ancient masonry. On the other hand, the CFRP mesh will provide to the reinforcement layer with the needed tensile strength. The main advantages [20] of using CFRP mesh instead of traditional steel meshes comes from its higher tensile strength, durability, ease of application, and thinner mortar layer (unlike steel meshes, CFRP mesh does not require a mortar cover to protect it from the environment).

The results of preliminary tests [21] showed that a traditional mortar coating application was not able to ensure proper bonding between the wall and the reinforcing render when the CFRP mesh resistance is fully exploited. An innovative application technology was then developed to ensure the needed bonding, based on the shotcrete technology (Fig. 2). As the coating mortar is applied by high-speed spraying to the masonry substrate, the adhesion levels [22] needed to bond the reinforcing render material to the masonry substrate is ensured [21].

Ordinary masonry walls are usually constituted by two contiguous layers, with poorer materials between them, which may present a tendency to split under the effect of compression and bending. To avoid the masonry split, especially when the connection between layers is poor or non-existent [5, 23, 24], the strengthening technique also considers the connection between both sides of the masonry walls through the installation of steel confinement devices. Those steel confinement devices, when properly placed, also ensure an enhanced bonding between the strengthening layer and the masonry wall. Such effect allows the CFRP mesh to be tensioned until its maximum strength is achieved, allowing the full exploitation of this material.

The anchoring at singular zones is fundamental to ensure the adequate behaviour of the strengthening layer. Such layer will only be effective if properly anchored at its endings, as well as at specific transitional zones where the layer is interrupted (for example across the building wooden floors). In the developed technique, such purpose is ensured mainly

Fig. 2 Render mortar shotcrete operation

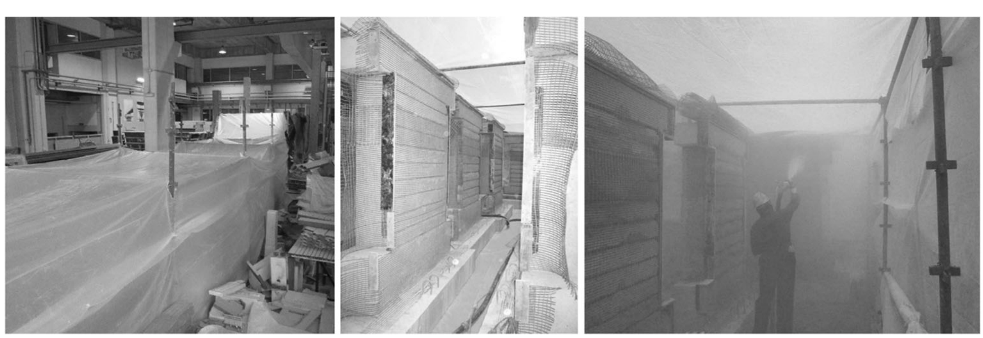

Table 1 Render mortar mechanical characterization [21]

		Uniaxial compressive strength		Young modulus	
Mortar ref.	Mortar solution (Manufacturer)	Averaged stress	Standard deviation	Averaged value	Standard deviation
MAP_01	Albaria Intonaco (BASF)	4.99 MPa	7.8%	0.83 GPa	1.6%
MAP_02	Reabilita Cal (SECIL)	4.62 MPa	1.2%	0.86 GPa	3.9%

with the organic adhesion (by epoxy resins) of the CFRP mesh to specific steel devices (Fig. 1b) that will ensure the anchoring requirements [21].

Material Characterization

The material characterization was directed at the determination of the main mechanical characteristics of the materials constituting the strengthening solution (the CRFP reinforced mortar), and those of the masonry test specimens used in the subsequent laboratory work.

The mortar matrix of the reinforced render material was mechanically characterised by uniaxial compression tests, where compression strength and Young's Modulus were determined. Mortars for non-structural rehabilitation of old masonry elements were considered adequate for the intended purposes, because of their mechanical and chemical compatibility. Because of logistical constraints, two different types of mortars had to be used, ensuring, however, that they presented a similar composition. For this purpose, several specimens of both types of sprayed mortars were prepared, from which cylindrical core samples (with Ø66 mm × 120 mm) were drilled for further testing.

The mortar samples were tested according to the procedures defined at EN 12390:3 [25] at 28 days of age (Table 1). As expected, both mortars presented quite similar mechanical characteristics.

As referred, masonry wall specimens were produced to test the effect of the proposed strengthening solution. Manually manufactured masonry walls usually present highly dispersed values of their mechanical and physical properties. For the required serial production of masonry wall specimens ensuring lower variability, a pseudo-masonry material was developed, in such a way that it could be considered mechanically equivalent to the masonry typically found in old buildings. This pseudo-masonry was homogeneous, while real masonry, in most cases, is marked by their masonry layers discontinuity. Since this morphology has a particular impact on high axial compression states, being less significant for moderate compression and bending forces, the decision of using a material of this kind turned out to be acceptable.

The pseudo-masonry material was composed of a mixture of clay-rich sand, river sand and coarse aggregate (gravel), bonded by a hydraulic lime binder, and produced at a concrete batching-plant. This material was mechanically characterised (Table 2) by uniaxial compression tests (performed to three samples for each pseudo-masonry manufacturing), according to EN 206:1 [26] and by tests to determine its Young modulus on Ø150 mm × 300 mm cylinders (performed on three samples for each manufacturing, with the exception of the PSA_07 pseudo-masonry), according the EN 12390:13 [27]. All tests were performed at 28 days of age. It is worth noting that PSA_07 pseudo-masonry was quite stronger then PSA_06, PSA_09 and PSA_10. Regarding the Young modulus, a higher dispersion of results was found, with values ranging between 2 GPa and 7 GPa.

Experimental Setup

A specific experimental setup was conceived to perform quasi-static testing with reversed cycles of horizontal displacements on the pseudo-masonry specimens. This setup was developed for the assessment of the seismic behaviour of physical models of masonry walls, both plain and strengthened.

Table 2 Pseudo-masonry mechanical characterization

	Uniaxial compressive strength		Young modulus	
Pseudo-masonry reference	Averaged stress	Standard deviation	Averaged value	Standard deviation
PSA_06	2.20 MPa	2.8%	2.10 GPa	0.1%
PSA_07	4.45 MPa	4.7%	–	–
PSA_09	2.00 MPa	4.9%	3.46 GPa	7.5%
PSA_10	2.97 MPa	2.1%	7.02 GPa	2.9%

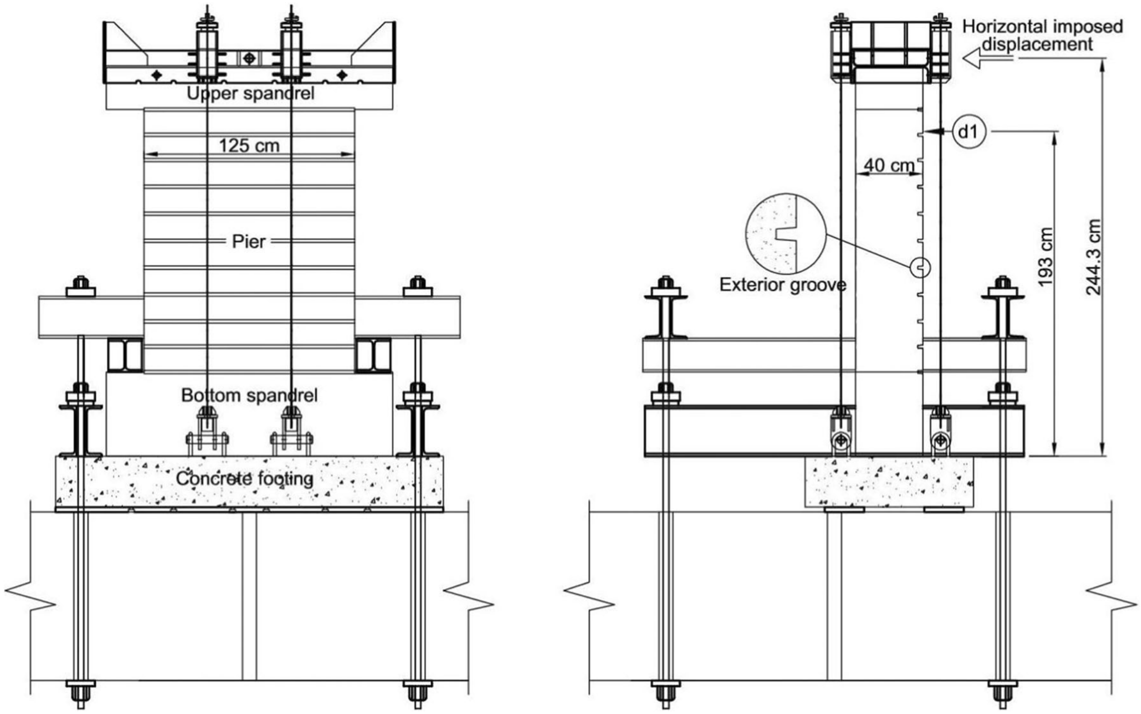

Fig. 3 Specimens geometry

The geometry of the specimens had to be representative of the walls of old masonry buildings. Therefore, they consisted of an upper spandrel, a pier and a bottom spandrel (Fig. 3). All masonry specimens were 40 cm thick, with small horizontal grooves. Such grooves simulate the superficial mortar joints removal that the strengthening technique may require to promote the adhesion between the masonry and the reinforcing mortar.

Two initial reference tests were performed to characterize the non-reinforced behaviour of the masonry walls specimens (non-reinforced specimens EPR_01 and EPR_02, Table 3), with different axial loading, following the test scheme presented in Fig. 4. The same test scheme led to the realization of eight tests to strengthened specimens (EPF_01 to EPF_08, Table 3).

The experimental campaign comprised the analysis of the influence of the main strengthening solution parameters on the structural behaviour of the masonry walls, namely the axial load applied, the reinforced render mortar matrix material and the presence of the confinement devices. Test specimens dimensions and strengthening details are shown in Table 3.

Two axial load levels were adopted defining an interval of axial stress levels corresponding to the most common values found in masonry walls for old buildings. A low load level (100 kN) corresponding to a compressive stress of 0.20 MPa in the specimen pier, and a moderate level of loading (200 kN) corresponding to an installed stress (in the pier) of 0.40 MPa, were then considered.

Table 3 Tests specifications

Test reference	*Pseudo-masonry*	Specimen geometry		Mortar solution	CFRP mesh (manufact.)	Confinement devices	Axial load
		Pier	Spandrels				
EPR_01	PSA_10	156 cm (height) X 125 cm (width)	Bottom: 50 cm (height) X 170 cm (width)	–	–	–	100 kN
EPR_02							200 kN
EPF_01	PSA_06			Albaria Intonaco	2 cross layers ARMO-mesh L500 (S&P)	Present (9 pairs applied on pier)	100 kN
EPF_02	PSA_07		Upper: 25 cm (height) X 170 cm (width)	Reabilita Cal			
EPF_03	PSA_06			Albaria Intonaco			200 kN
EPF_04	PSA_07			Reabilita Cal			
EPF_05	PSA_09			Reabilita Cal		Absent	100 kN
EPF_06							
EPF_07	PSA_06			Albaria Intonaco			200 kN
EPF_08	PSA_09			Reabilita Cal			

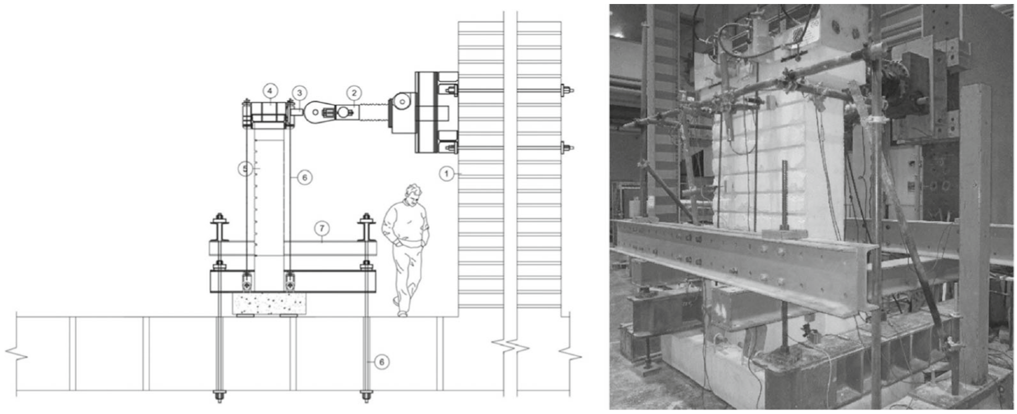

1 Reaction wall

2 Hydraulic jack

3 Load cell

4 Steel helmet

5 Pseudo-masonry specimen

6 Dywidag bar

7 Restraining steel structure

Fig. 4 Test setup

To prevent rigid-body failure mechanisms the bottom spandrels displacement was restrained by a steel structure. The reversed cyclic pseudo-static horizontal loading was applied using a screw jack connected to a steel helmet involving the upper spandrels. The screw jack axis, which imposed the cyclic horizontal displacement, was positioned 244.3 cm above the concrete footing (Fig. 3). The axial (vertical) load was applied by using four externally tensioned Dywidag bars, connected to the steel helmet and to the concrete footing. These Dywidag bars were tensioned with active controlled hydraulic jacks that maintained the applied load during the test, avoiding variations that would influence the results.

The CFRP reinforcing mesh was anchored to the concrete footing only after the axial load was installed. This corresponds to real situations, were the walls are permanently subjected to self-weight loading. The application of the confinement devices (Fig. 5) followed the same precaution.

The horizontal out-of-plane tests with reversed cycles allowed observing the specimen behaviour when the reinforcement is tensioned and when it is compressed. The displacement cycle history (Fig. 6) was defined following ASTM E2126:05 [28]. A cyclic history matching the Scheme B of that standard was adopted. The failure criteria corresponded to the situation when the horizontal load developed on the last cycle is 20% (or more) lower than the peak load achieved in the preceding steps. The adopted history of the imposed displacements is depicted in Fig. 6. The applied displacement d1 was measured 193 cm above the concrete footing, as shown in Fig. 3.

Experimental Results

An overview of the experimental results is reported in Table 4. This table shows the d1 displacement (Fig. 3) and drift (d1/193 cm) corresponding to the maximum load achieved, as well as the corresponding bending moment at the pier cross-section adjacent to the bottom spandrel. For each test, the overall dissipated energy is also presented. The positive loading direction (indicated as "PULL (+)" in Table 4) corresponds to tensioning in the reinforced render.

Reference Specimens

The deformation capacity is one of the main parameters regarding the collapse behaviour of masonry walls when subjected to earthquakes. Unlike masonry walls, which usually

Fig. 5 Tests assemblage

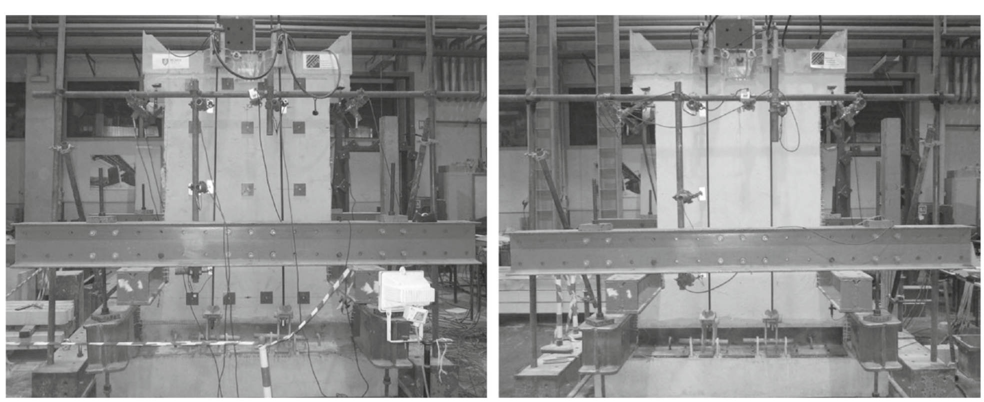

(a) Using confinement devices **(b)** Without confinement devices

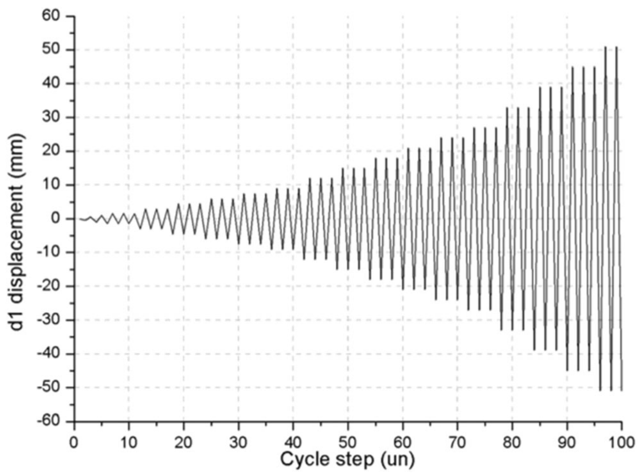

Fig. 6 Theoretical loading cycle of the quasi-static testing of reversed cycles of horizontal displacements

present out-of-plane brittle behaviour (with increasing brittleness as the wall height increases), EPR_01 and EPR_02 specimens presented a pseudo-ductile load-displacement diagram, with a horizontal plateau (Fig. 7a). Although the reference specimens EPR_01 and EPR_02 (Fig. 7a) did not meet the defined failure criterion, they would have reached the limit load-bearing capacity in a practical situation, or if the test scheme allowed the unconstrained collapse of these specimens.

Regarding the specimens damage patterns, the most evident was the formation of a horizontal crack slightly above the transition section (between the pier and the bottom spandrel), which eventually extended through the entire wall thickness (Fig. 7b), due to the alternate imposed displacements. The cracked section eventually behaved as a hinge leading to the specimen's rigid-body motion, by opening and closing its gap (Fig. 7b). When this hinge behaviour was reached, the wall showed no further capacity to support out-of-plane loads. Such cracks can hereby be defined as *hinge cracks* and after their formation they assumed the control of the behaviour of the non-reinforced specimens (rigid-body motion).

To define the collapse load and displacement values of each reference test, each cyclic range defined in the load history was individually analysed (Fig. 6). The collapse load corresponds to the maximum force achieved during the test. The collapse displacement corresponds to the displacement value observed when the maximum load was achieved for the first time after the hinge was formed.

In the case of the reference specimen EPR_01, tested with a low axial load (100 kN), the pulling collapse (positive displacements) occurred for a displacement of approximately 15 mm and a load value of about 14 kN (Fig. 8). The pushing collapse (negative displacements) occurred for a displacement of approximately 15 mm and a load value of about 12 kN (Fig. 8).

Table 4 Tests results overview

Test reference	Loading direction	Maximum load	Bending moment	Displacement d1 at maximum load	Drift at maximum load	Test dissipated energy (J)
EPR_01	PULL (+)	14.4 kN	28,0 kN.m	14.8 mm (*)	0,76% (*)	4490
	PUSH (−)	12.8 kN	24,9 kN.m	4.0 mm (*)	0,20% (*)	
EPR_02	PULL (+)	22.2 kN	43,1 kN.m	31.4 mm (*)	1,61% (*)	6135
	PUSH (−)	21.4 kN	41,6 kN.m	16.8 mm (*)	0,86% (*)	
EPF_01	PULL (+)	37.6 kN	73,1 kN.m	33.9 mm	1,74%	8066
	PUSH (−)	15.3 kN	29,7 kN.m	13.2 mm	0,68%	
EPF_02	PULL (+)	44.1 kN	85,7 kN.m	50.4 mm	2,59%	9224
	PUSH (−)	19.5 kN	37,9 kN.m	14.1 mm	0,73%	
EPF_03	PULL (+)	39.8 kN	77,3 kN.m	33.3 mm	1,71%	13,911
	PUSH (−)	24.8 kN	48,2 kN.m	15.8 mm	0,81%	
EPF_04	PULL (+)	48.3 kN	93,9 kN.m	49.3 mm	2,54%	10,175
	PUSH (−)	31.5 kN	61,2 kN.m	22.2 mm	1,14%	
EPF_05	PULL (+)	32.3 kN	62,8 kN.m	31.4 mm	1,62%	5268
	PUSH (−)	14.6 kN	28,4 kN.m	12.8 mm	0,66%	
EPF_06	PULL (+)	30.3 kN	58,9 kN.m	33.0 mm	1,70%	7603
	PUSH (−)	16.0 kN	31,1 kN.m	17.8 mm	0,92%	
EPF_07	PULL (+)	42.0 kN	81,6 kN.m	44.1 mm	2,27%	11,837
	PUSH (−)	22.4 kN	43,5 kN.m	18.5 mm	0,95%	
EPF_.08	PULL (+)	40.5 kN	78,7 kN.m	47.9 mm	2,46%	11,721
	PUSH (−)	24.5 kN	47,6 kN.m	17.9 mm	0,92%	

(*) The failure criterion was not achieved

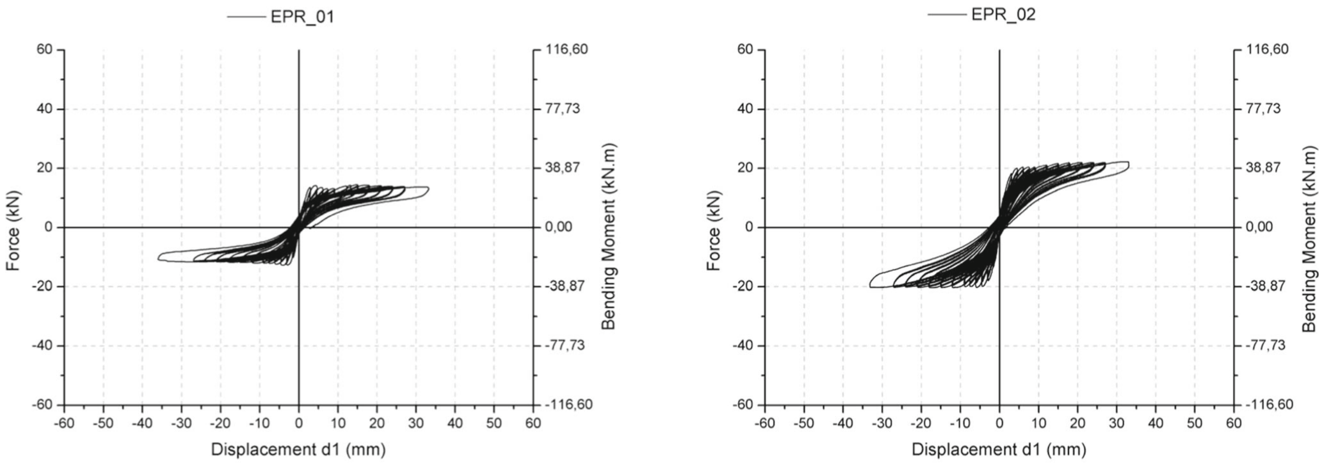

(a) Load-displacement curves

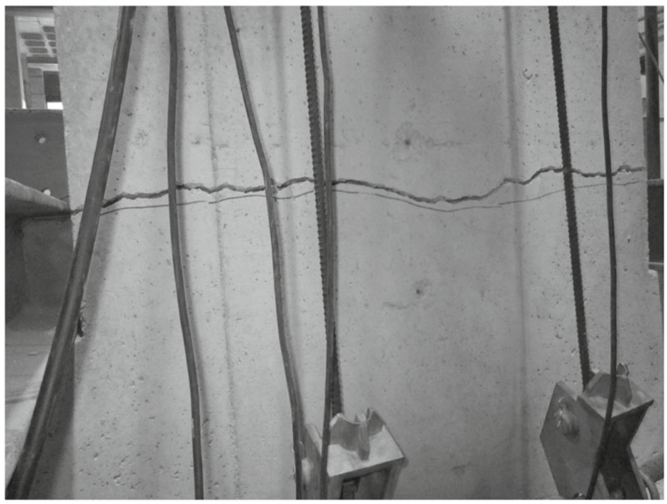

(b) Crack pattern (EPR_01 specimen)

Fig. 7 Tests to EPR_01 and EPR_02 specimens

Regarding the reference specimen EPR_02, tested with a moderate axial load (200 kN), the pulling collapse occurred for a displacement of approximately 18 mm and a load value of about 22 kN (Fig. 9), while the pushing collapse occurred for a displacement of approximately 18 mm and a load value of about 20 kN (Fig. 9).

Strengthened Specimens

For EPF_01 and EPF_02 strengthened specimens the collapse was caused by the ripping of the reinforced render CFRP mesh, leading to a significant decrease in the specimens bearing capacity. The damage found on the pseudo-masonry was mainly due to the bending out-of-plane mechanism, associated to the formation of several horizontal bending cracks (Fig. 10a). The lower crack (in the transition section between the wall pier and its bottom spandrel) crossed the entire width of the specimen for negative displacements (causing compression in the reinforcement layer). For positive displacements, the tensioned CFRP reinforcement led to a distributed crack behaviour instead of a rigid-body motion.

For EPF_05 and EPF_06 specimens (without confinement devices) the collapse mode (damage patterns) involved the debonding between the CFRP reinforced render and the masonry. This led to the absence of some of the flexural distributed cracks, as the detachment of the reinforced render layer occurred before these cracks could develop and before the CFRP mesh rupture. Notwithstanding the separation between masonry substrate and the reinforced render layer (Fig. 10b), the reinforcement continued to provide significant bending capacity to the wall, leading to only slightly lower maximum horizontal loads and similar deformation capacity, when compared to those obtained in the specimens with confinement devices (Table 4, Fig. 11).

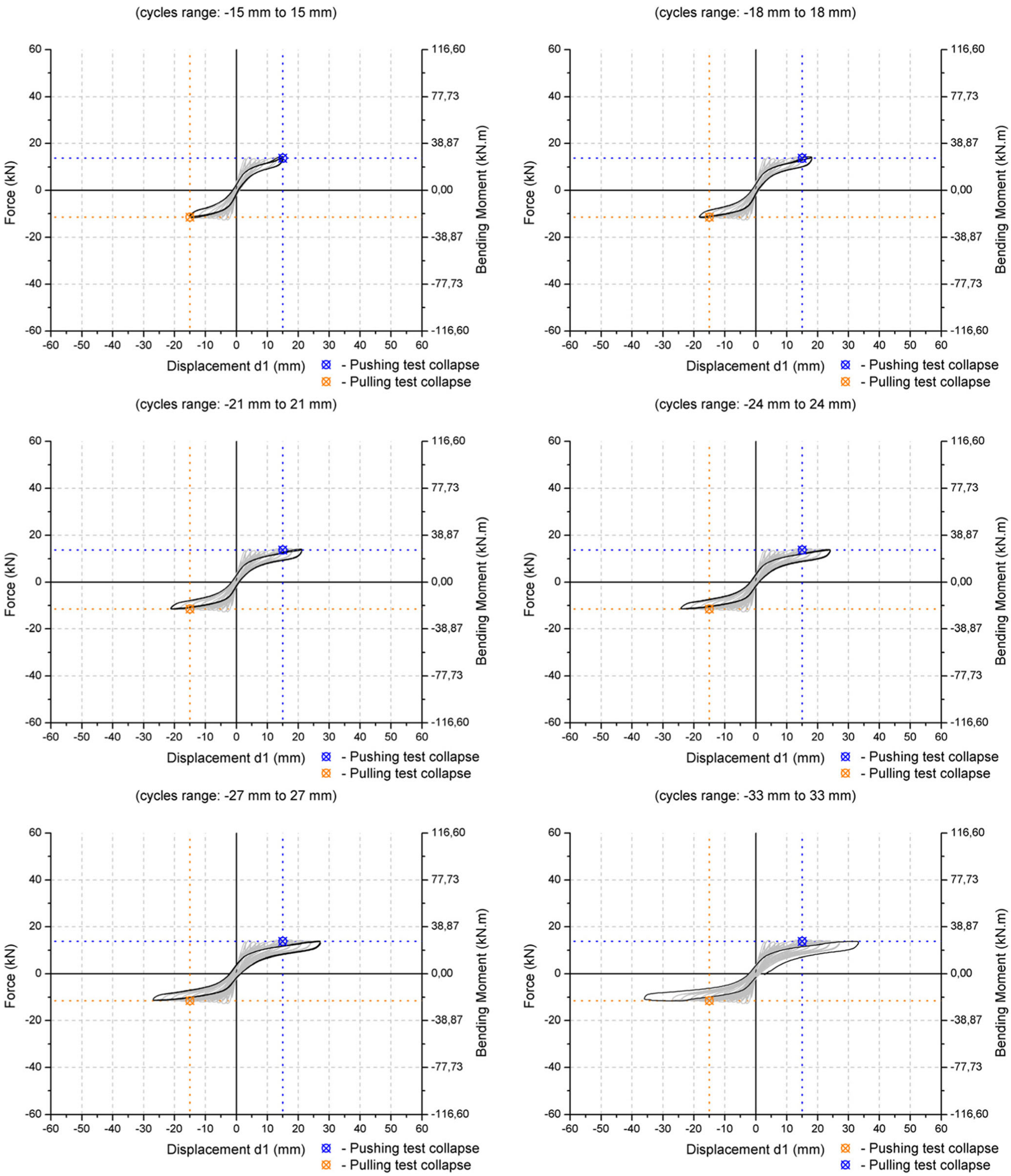

Fig. 8 EPR_01 failure collapse definition (low axial load: 100 kN)

For the strengthened specimens with the low axial load (EPF_01, EPF_02 and EPF_05, EPF_06) a considerable increase in the flexural out-of-plane strength was noticed for positive displacements, when the CFRP reinforced render was tensioned (Table 4, Fig. 11).

For positive displacements, the strengthened specimens with a low axial load showed an increasing path in the diagram (Fig. 11), instead of the plateau of the reference specimens. The evaluation of the deformation capacity improvement was based in the comparison between displacement d1

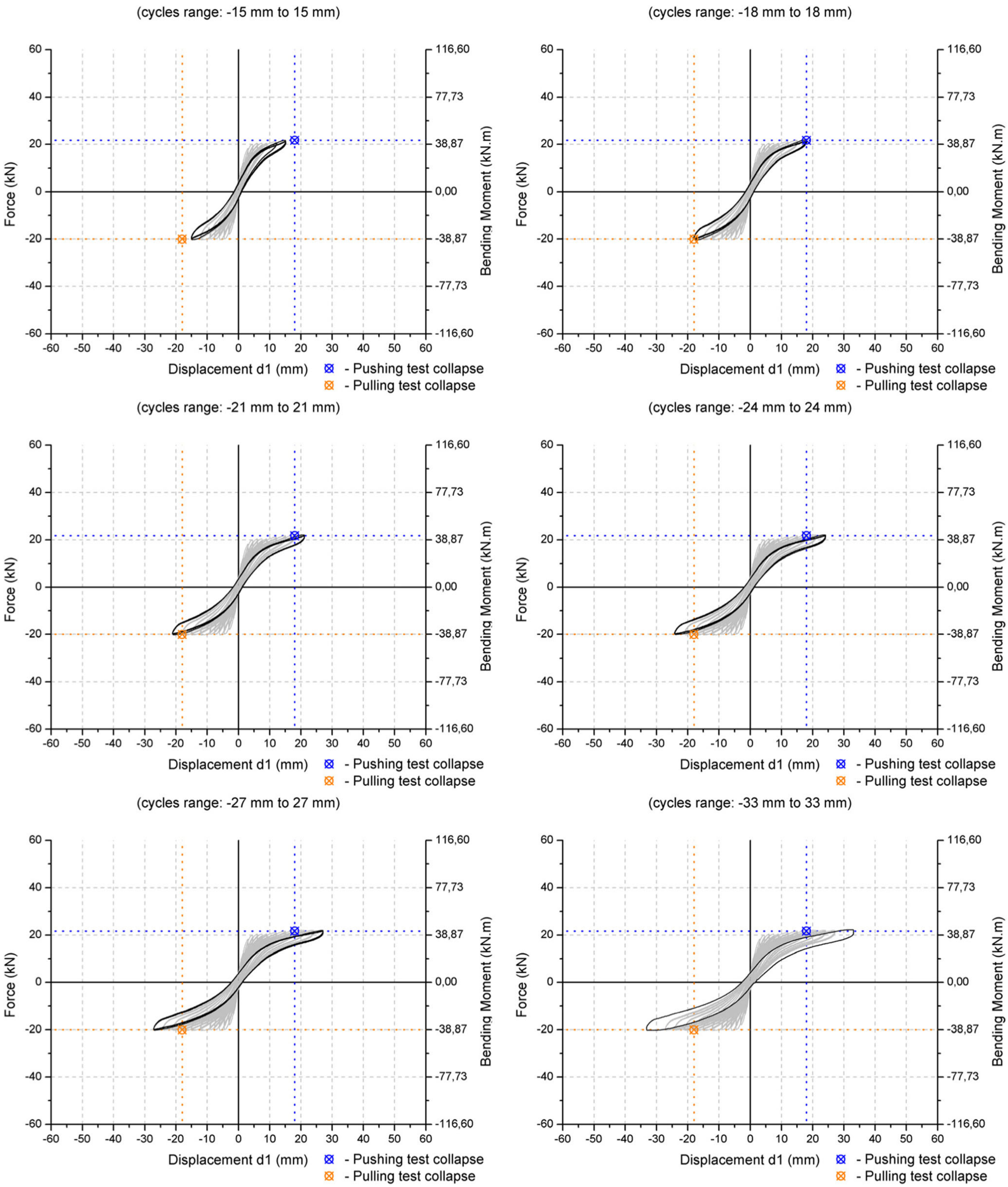

Fig. 9 EPR_02 failure collapse definition (moderate axial load: 200 kN)

(or the drift) corresponding to the pull and push collapse loads and the same parameter referred to reference test of EPR_01 (Fig. 8). When the CFRP reinforced render was tensioned a major increase in the deformation capacity was observed, as well as in the collapse load (Fig. 11) when compared to those of the reference test (EPR_01).

When the reinforcement layer was compressed (negative displacements), no significant increase in both deformation

Fig. 10 Damage patterns for the tests with low axial load (100 kN)

(a) Crack pattern (EPF_01 specimen)

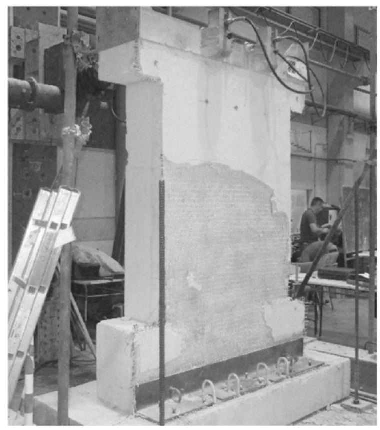

(b) CFRP reinforced render detachment (EPF_06 specimen)

capacity and strength were noticed, when compared to those observed for positive displacements (Table 4, Fig. 11).

The axial load increase (200 kN) did not lead to significant differences when compared to the results achieved with a lower axial load (100 kN), as maximum horizontal loads and corresponding displacements were only slightly improved. Again, with a moderate axial load of 200 kN (EPF_03, EPF_04 and EPF_07, EPF_08 specimens) the reinforcing render led to considerable increase in strength and deformation capacity for positive displacements (Table 4, Fig. 12), in comparison with the reference test (EPR_02 specimen). Those improvements were again insignificant for negative displacements (when compressing the reinforced render layer).

For a moderate level of axial load (200 kN) the damage pattern kept the same features than for the low axial load (100 kN). Again, the tension resistance of the CFRP mesh was fully exploited as the collapse was always associated to the tension rupture of this material.

The pseudo-masonry used in specimens EPF_02 and EPF_04 (PSA_07) was markedly stronger than real masonry (Table 2). The maximum positive and negative loads obtained in these tests should have been somewhat blistered when compared to the tests with typical masonry mechanical properties.

Overall Remarks

The out-of-plane collapse of the non-strengthened wall specimens mainly displayed the damage normally found in common masonry walls subjected to earthquakes, which is typically associated with the formation of horizontal tensile *hinge cracks* (joints), caused by bending.

The strengthened specimens exhibited similar overall out-of-plane bending collapse mechanisms but involved other damage, which determined the masonry's bearing capacity to out-of-plane bending, namely:

- Rupture of the CFRP mesh of the reinforcement layer, when tensioned;
- Formation of a group of distributed horizontal bending cracks, opened only when the reinforcement layer was tensioned;

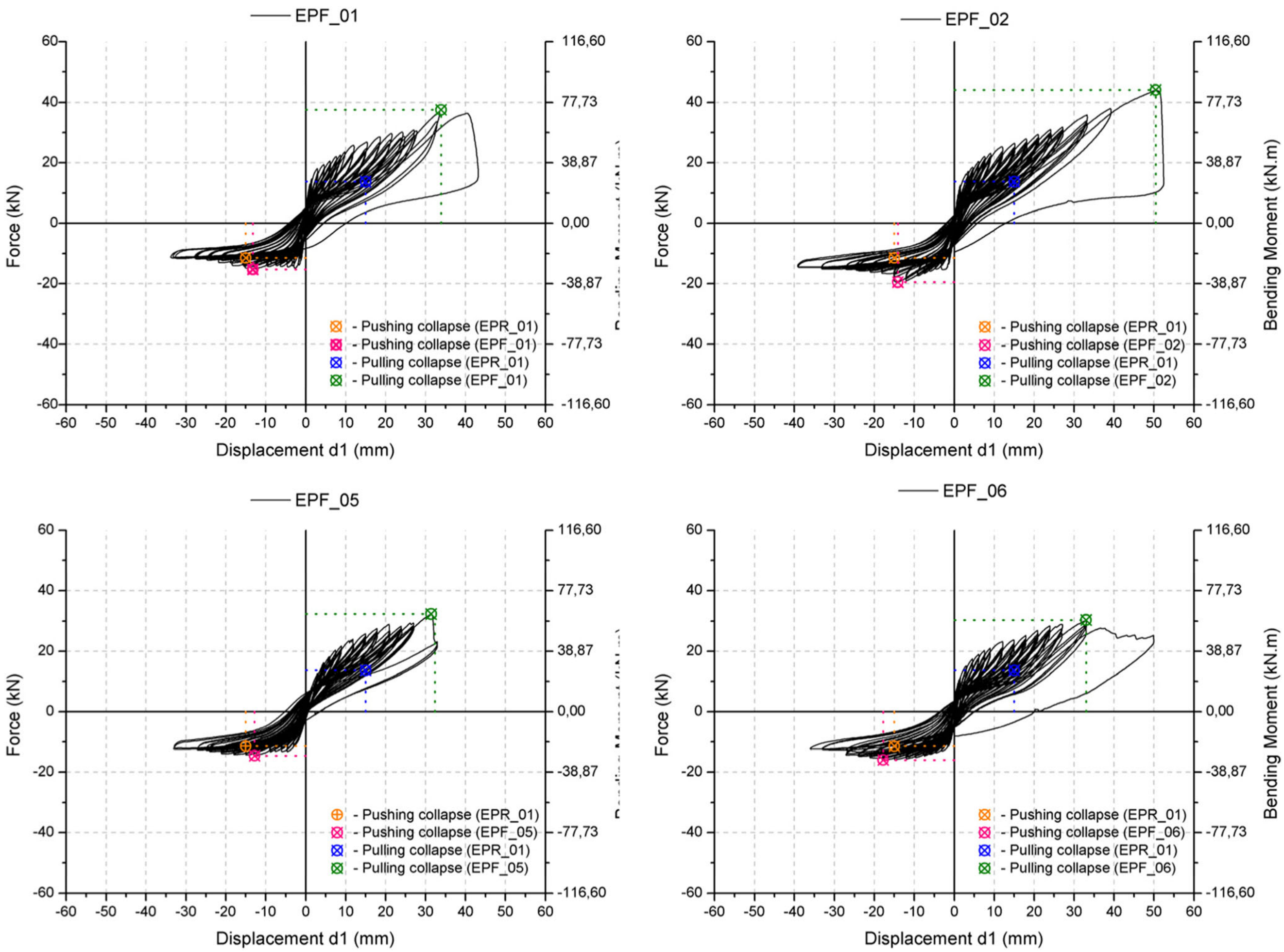

Fig. 11 Load displacement curves for the tests with low axial load (100 kN)

- CFRP reinforced render detachment (only observed when the confinement devices were absent).

By increasing the axial load applied on the specimen, their capacity to resist horizontal out-of-plane actions is not significantly enhanced. This suggests some limitations due to excessive compression in the pseudo-masonry material, which has not been sufficient to lead to the specimen's collapse, since the snap of the CFRP mesh still occurred.

Finally, the effect of the strengthening technique in the walls stiffness, deformation capacity and energy dissipation was also evaluated. The comparison between the specimens' initial ("elastic") stiffness in plain and strengthened walls was analysed in the cycles performed soon before collapse, ranging from −33 mm to 33 mm (Fig. 13).

Reference specimens (EPR_01 and EPR_02) were of a stiffer pseudo-masonry (PSA_10, Table 2), thus explaining the higher stiffness obtained at their tests. Table 5 presents the initial stiffness values obtained in the different tests, for both positive and negative displacements. The results of the EPF_02 and EPF_04 specimens are not shown, because its pseudo-masonry Young modulus was not measured (Table 2).

In the strengthened specimens, the initial stiffness for positive (tension of the reinforcement) and negative (compression of the reinforcement) displacements were practically the same (Table 5), showing that the reinforcement acts only for higher displacements. This behaviour demonstrates the high compatibility between the specimen material and the CFRP reinforced render reinforcement.

The results have shown that the walls strengthening strongly increased their deformation capacity for positive displacements (tensioned reinforcement, Figs. 11 and 12). Furthermore, the reinforcement also proved to avoid rigid-body out-of-plane motion (Figs. 7a and 14), that corresponds to a critical collapse mode in old buildings subjected to earthquakes, especially for higher ones.

Regarding the energy dissipation capacity, an important increase was also observed in the strengthened walls (Fig. 15), provided by the distributed cracking

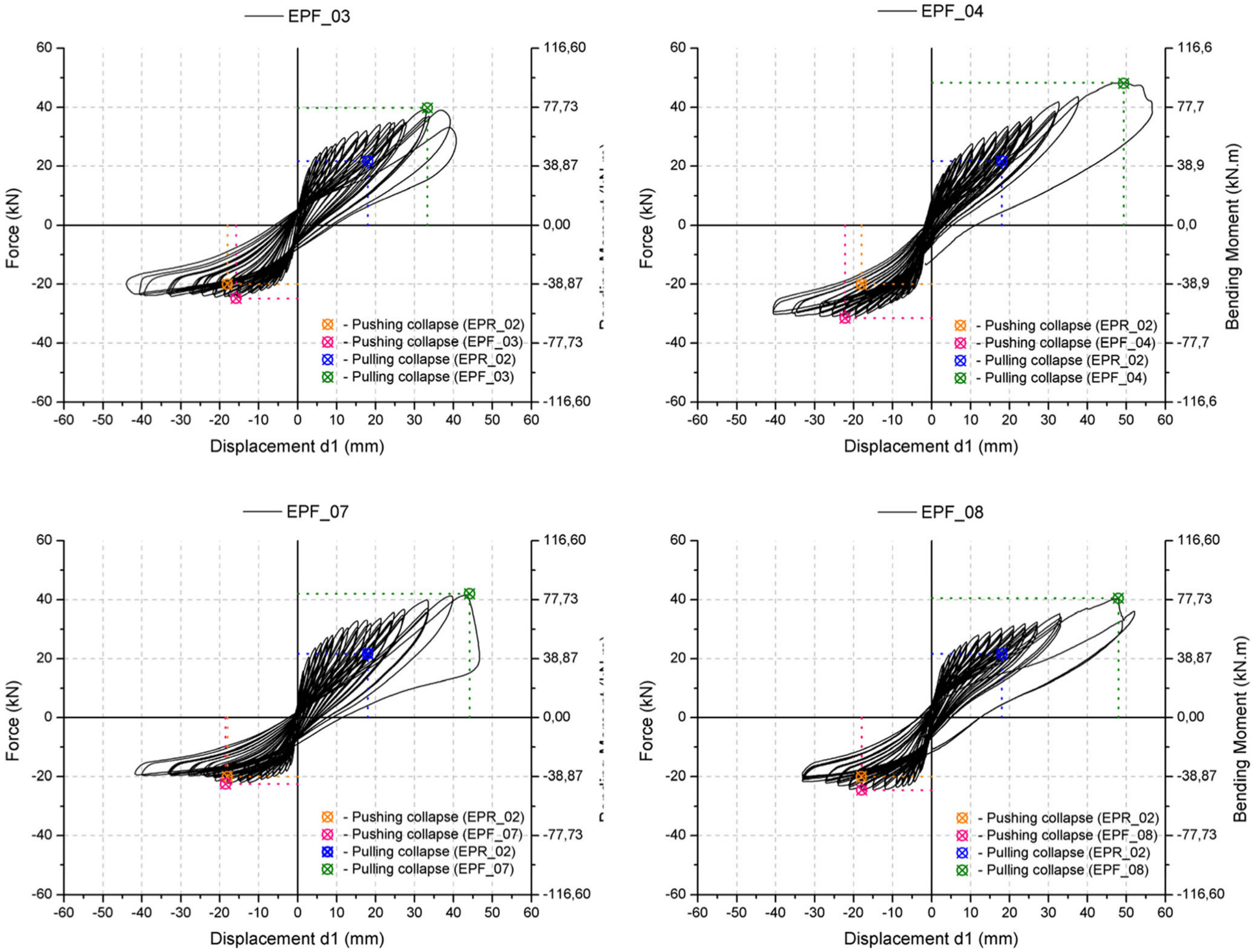

Fig. 12 Load displacement curves for the tests with moderate axial load (200 kN)

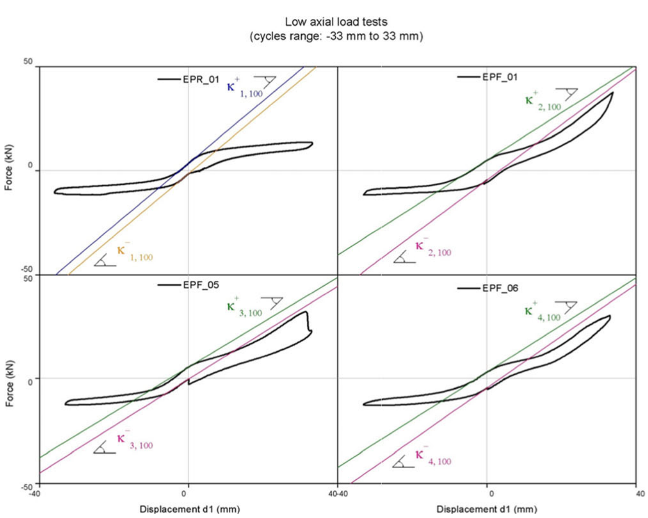

(a) Low axial load (100 kN)

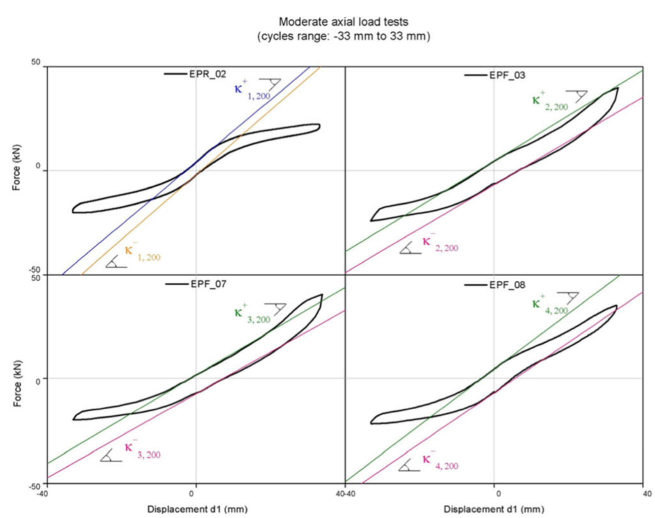

(b) Moderate axial load (200 kN)

Fig. 13 Test specimens stiffness (cyclic range from −33 mm to 33 mm)

Table 5 Specimens stiffness (at cyclic range − 33 mm to 33 mm)

Test reference	EPR_01	EPF_01	EPF_05	EPF_06	EPR_02	EPF_02	EPF_07	EPF_08
Axial load	100 kN				200 kN			
Stiffness (kN/m)	$k^+_{1,100}$	$k^+_{2,100}$	$k^+_{3,100}$	$k^+_{4,100}$	$k^+_{1,200}$	$k^+_{2,200}$	$k^+_{3,200}$	$k^+_{4,200}$
	1500	1145	1082	1138	1500	1093	1057	1343
	$k^-_{1,100}$	$k^-_{2,100}$	$k^-_{3,100}$	$k^-_{4,100}$	$k^-_{1,200}$	$k^-_{2,200}$	$k^-_{3,200}$	$k^-_{4,200}$
	1500	1334	1138	1249	1556	1055	1028	1214

induced by the reinforcement CFRP mesh. The load-displacement diagrams enveloped by the strengthened specimens tests show wider hysteretic cycles than those of the non-strengthened specimens (Fig. 14), especially in the later imposed displacements that these specimens could not achieve.

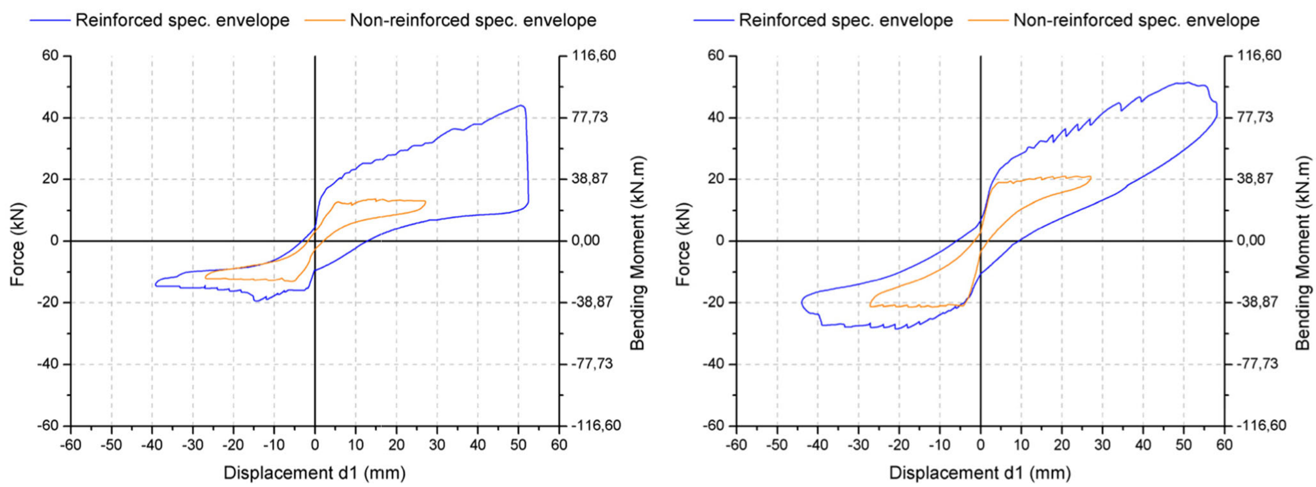

(a) Low axial load (100 kN) **(b)** Moderate axial load (200 kN)

Fig. 14 Load-displacement curves envelopes

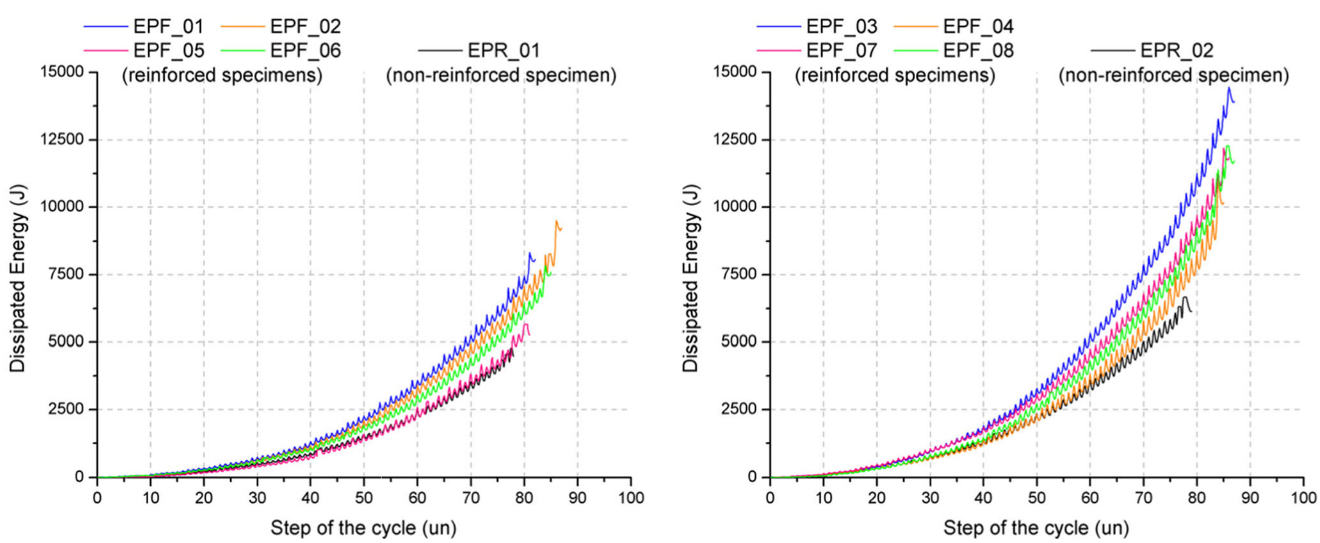

(a) Low axial load (100 kN) **(b)** Moderate axial load (200 kN)

Fig. 15 Experimental dissipated energy results

Conclusions

The research developed aimed at proposing a strengthening technique to improve the structural behaviour of masonry walls in old buildings.

The proposed technique consists of applying a non-cementitious render layer with a reinforcing CFRP mesh anchored at the ends with steel devices and, possibly, complemented with confinement devices.

The experimental study carried out demonstrates that the proposed strengthening technique significantly improves the behavioural parameters of the structural masonry walls of old buildings. The strength increase achieved is notorious, as well as the deformation capacity and the energy dissipation improvements, these two latter aspects being particularly important for masonry walls when subjected to out-of-plane actions [29].

The experimental tests analysis constitute an adequate basis for the definition of a technical guideline as comprehensive as possible for the application and dissemination of the strengthening technique. An extensive numerical work is also completed, allowing for the dimensioning of the reinforcement design. The main conclusions of this work will be available on future publications of the same authors.

Acknowledgements The authors gratefully acknowledge STAP, S.A, promoter of the R&D project Rehab Toolbox, sponsored by FEDER through the POR Lisboa – QREN – Sistemas de Incentivos I&DT, for allowing the disclosure of the data presented in this paper.

The authors also gratefully acknowledge the participation of S&P, S.A in the same R&D project.

The authors would like to thank the Ministério da Ciência, Tecnologia e Ensino Superior (Ministry of Science, Technology and Higher Education), FCT, Portugal [grant number SFRH/BD/79339/2011].

References

1. Lagomarsino S, Brencich A, Bussolino F, Moretti A, Pagnini L, Podestà S (1997) Una nuova metodologia per il rilievo del danno alle chiese: prime considerazioni sui meccanismi attivati dal sisma. Ingegneria Sismica; No. 3
2. Binda L, Gambarotta L, Lagomarsino S, Modena C (1999) A multilevel approach to the damage assessment and seismic improvement of masonry buildings in Italy. CRC press / Balkema; seismic damage to masonry buildings; Rotterdam, The Netherlands
3. Borri A, Avorio A, Cangi G (1999) Considerazioni sui cinematismi di collasso osservati per edifici in muratura. IX Convegno Nazionale "L'ingegneria Sismica in Italia", ANIDIS; Turin, Italy
4. D'Ayala D (1999) Correlation of seismic vulnerability and damages between classes of buildings: churches and houses, in seismic damage to masonry buildings. CRC press / Balkema; seismic damage to masonry buildings; Rotterdam, The Netherlands
5. Giuffrè A (1993) Sicurezza e conservazione dei centri storici in area sismica, il caso Ortigia. Editora Laterza; Bari
6. Doglioni F, Moretti A, Petrini V (1994) Le chiese ed il terremoto. Editoriale Lint; Trieste
7. Binda L, Baronio G, Gambarotta L, Lagomarsino S, Modena C (1999) Masonry constructions in seismic areas of central Italy: a multi-level approach to conservation. VIII north American masonry conference - 8NAMC; Austin
8. D'Ayala D, Speranza E. (1999) Identificazione dei meccanismi di collasso per la stima della vulnerabilità sismica di edifici nei centri storici. IX Convegno Nazionale "L'ingegneria Sismica in Italia", ANIDIS; Turin
9. Zuccaro G, Papa F. (2003) CD Multimediale MEDEA - Manuale di Esercitazioni sul Danno Ed Agibilità per edifici ordinari in muratura. Dipartimento Protezione Civile; Rome
10. Borri A, Cangi G (2004) Vulnerabilità ed interventi di prevenzione sismica nei centri storici umbri dell'alta Val Tiberina. XI Congresso Nazionale "L'ingegneria Sismica in Italia", ANIDIS; Genoa
11. Doglioni F (1999) Codice di pratica (linee guida) per la progettazione degli interventi di riparazione, miglioramento sismico e restauro dei beni architettonici danneggiati dal terremoto umbro-marchigiano del 1997. Bollettino Ufficiale della Regione Marche
12. Costa A, Penna A, Arêde A, Costa A (2015) Simulation of masonry out-of-plane failure modes by multi-body dynamics. Earthq Eng Struct Dyn. https://doi.org/10.1002/eqe.2596
13. Ferreira T, Costa A, Arêde A, Varum H, Costa A (2016) In-situ out-of-plane testing of original and strengthened traditional stone masonry walls using airbags. J Earthq Eng 20:749–772. https://doi.org/10.1080/13632469.2015.1107662
14. Poletti E, Vasconcelos G, Jorge M (2015) Application of near surface mounted (NSM) strengthening technique to traditional timber frame walls. Constr Build Mater 76:34–50. https://doi.org/10.1016/j.conbuildmat.2014.11.022
15. Ferreira J, Teixeira M, Dutu A, Branco F, Gonçalves M (2012) Experimental Evaluation and Numerical modelling of timber-framed walls. Exp Tech 38:45–53. https://doi.org/10.1111/j.1747-1567.2012.00820.x
16. Binda L, Anzani A, Cantini L, Cardani G, Tedeschi C, Saisi A (2006) On site and laboratory investigation on some churches hit by a recent earthquakes, in Order to assess the damages to materials and structures. I international conference on restoration of heritage masonry structures; Cairo
17. Avorio A, Borri A, De Maria A (2002) Sisma umbro-marchigiano del settembre 1997 e successivi a Sellano: comportamento di una schiera di edifici consolidati. Ingegneria Sismica 2:54–71
18. Drei A, Milani G, Sincraian G (2017) DEM numerical approach for masonry aqueducts in seismic zone: two valuable Portuguese examples. Int J Masonry Res Innov 1(2). https://doi.org/10.1504/IJMRI.2017.082392
19. Dutu A, Ferreira J, Sandu C (2013) Incremental seismic rehabilitation concept for Romanian civil buildings integrated in natural hazards prevention management. Int J Emerg Manag 9(3):248–257. https://doi.org/10.1504/IJEM.2013.058545
20. Ismail A, Ingham J (2016) In-plane and out-of-plane testing of unreinforced masonry walls strengthened using polymer textile reinforced mortar. Eng Struct 118:167–177. https://doi.org/10.1016/j.engstruct.2016.03.041
21. Guerreiro J, Proença M, Ferreira J, Gago A. (2017) Bonding and anchoring of a CFRP reinforced render for external strengthening of old masonry buildings. Construction and Building Materials. Under review
22. Colen I, Brito J, Branco F (2008) Situ adherence evaluation of coating materials. Exp Tech 33:51–60. https://doi.org/10.1111/j.1747-1567.2008.00372.x
23. Giaretton M, Dizhur D, Porto F, Ingham Z (2015) Constituent material properties of New Zealand unreinforced stone masonry buildings. J Building Eng 4:75–85. https://doi.org/10.1016/j.jobe.2015.08.005

24. Gago A, Proença A, Cardoso J, Cóias V, Paula R (2009) Seismic strengthening of stone masonry walls with glass fiber reinforced polymer strips and mechanical anchorages. Exp Tech 35:45–53. https://doi.org/10.1111/j.1747-1567.2009.00544.x
25. EN 12390:3. (2009) Testing hardened concrete; Part 3: Compressive strength of test specimens
26. EN 206:1. (2000) Concrete. Specification, performance, production and conformity
27. EN 12390:13. (2013) Testing hardened concrete. Part 13: Determination of secant modulus of elasticity in compression
28. ASTM E2126:05. (2005) Standard Test Methods for Cyclic (Reversed) Load Test for Shear Resistance of Walls for Buildings
29. Gonçalves AM, Gomes-Ferreira J, Guerreiro L, Branco F (2014) Seismic retrofitting of timber framed walls. Mater Constr 64(316): e040. https://doi.org/10.3989/mc.2014.06913